

# LASER SURFACE ALLOYING (LSA) OF ALUMINIUM (AA 1200) WITH TiB<sub>2</sub> FOR HARDNESS IMPROVEMENT

Paper (802)

Abimbola Patricia Popoola<sup>1\*</sup>, Sisa Pityana<sup>1,2</sup>

<sup>1</sup>Department of Chemical and Metallurgical Engineering, Tshwane University of Technology, P.M.B X680, Pretoria, South Africa.

<sup>2</sup>Center for Scientific and Industrial Research – National Laser Centre, P.O. Box 395, BLD 46F, Pretoria, South Africa, 0001.

## Abstract

The present work deals with the development of Aluminium metal matrix composite (MMC) using TiB<sub>2</sub> reinforcement. The aim is to improve the microhardness property of the substrate. The surface of the aluminium was sand blasted to improve its laser energy absorption and simultaneous deposition of the ceramic powder onto the surface of the substrate was carried out using a Rofin Nd: YAG laser with an Argon shield environment to prevent oxidation. The laser processing parameters were varied. The characterization of the alloyed surfaces MMC was carried out by Optical Microscopy (OPM), Scanning Electron Microscopy (SEM) and X-ray Diffraction (XRD). The microstructure of the alloyed layer shows that the ceramic powder was well dispersed within the Al-matrix. Good metallurgical bonds were evident. Microhardness measurements were carried out. The maximum depth attained was 1.17 mm. There was a microhardness increase from that of substrate which is 24±0.4 HV to that of the MMC layer 58.0±0.2 HV.

## Introduction

Aluminium and its alloys are remarkable for their excellent mechanical strength, low specific weight, and relatively low cost, and thus are widely used in industrial applications. The high strength to weight ratio of light metals and their alloys makes them widely used in various machinery and transportation systems [1,2]. Aluminium alloys are not hard enough to be used in many engineering applications especially where wear resistance and high loading conditions are compulsory material property requirements [1,3]. The hardening effects by conventional heat treatments through phase transformation are very limited since Aluminium is not one of the allotropic metals.

Laser surface alloying can be utilized for modification of the surface properties of metallic

alloys. This method has been applied for producing metal matrix composite MMC by many researchers [1,2,4]. MMC produced by LSA is achieved by the application of a laser beam on the surface of the substrate material to form a melt pool and then the injection of a powder material into the melt pool. The properties of laser surface alloyed layer depend on microstructure that evolves during melting, cooling and solidification, however, the application and efficiency of laser surface treatments depend on laser processing parameters [1,3].

Titanium diboride (TiB<sub>2</sub>) is a refractory material; it exhibits high elastic modulus and hardness, high melting point (2970°C) and electrical conductivity as well as good thermal stability and chemical inertness. TiB<sub>2</sub> has a good thermodynamic stability in Aluminium, hence the reason for its choice as alloying material in this work.

In this investigation, the effects of TiB<sub>2</sub> reinforcement on the microhardness property of Al will be studied, an accurate characterization of the alloyed layer MMC in terms resultant microstructures and phases will be carried out.

## Experimental approach

### Materials

The base material used in the current investigation is Aluminium AA 1200. The aluminium plates were cut and machined to dimensions 100 x 100 x 6 mm. The chemical composition of the substrate is shown in Table 1. The pure Al -plates were sand blasted prior to laser surface alloying to achieve a uniform rough surface which in turn enhances laser energy absorption at the surface of the Al -plates and also the removal of the oxide scale. The alloying powder used was TiB<sub>2</sub> (99.5%). The powder particle sizes range from -100 to 45 µm.

Table 1 Composition of AA 1200 alloy

Element	Composition by wt.%
Fe	0.59
Cu	0.12
Si	0.13
Al	balance

A Rofin Sinar continuous wave Nd: YAG solid-state laser fitted with off-axes nozzle used for powder feeding was used for laser surface alloying experiment. A Kuka robot was used to deliver the laser beam through a 600  $\mu\text{m}$  optical fiber to the target surface. The shielding gas used was Argon; this prevents oxidation of metal through reaction with oxygen and also avoids formation of pores that occurs during the alloying process. The processing parameters were optimized by variation and careful selection of the laser processing parameters. The laser parameters used are shown in Table 2. The laser power was held constant while the scan speed was varied during these experimental investigations. Single laser tracks were made on the substrate's surface.

Table 2 Laser processing parameters and sample composition

Sample label	C	D
System composition	Al-TiB <sub>2</sub>	Al-TiB <sub>2</sub>
Laser power (kW)	4.0	4.0
Beam diameter (mm)	3.0	3.0
Scan speed (m/min)	0.6	1.0
Powder feed rate (rpm)	4.0	4.0
Shielding gas	Argon	Argon
Shielding gas flow (L/min)	4.0	4.0

### Materials Characterisation

A Philips PW 1713 X-ray diffractometer fitted with a monochromatic Cu K $\alpha$  radiation set at 40 kV and 20 mA was used to determine the phase composition of powder. The scan was taken between 10° and 80° two theta (2 $\theta$ ) with a step size of 0.02 degree. Phase identification was done using Philips Analytical X'Pert HighScore® software with an in-built International Centre for Diffraction Data (ICSD) database. The powder particle morphology and size distribution were analyzed using a scanning electron microscope SEM equipped with energy dispersive spectrometer and Malvern Mastersizer 2000 image analyser for particle size.

Cross-sections of the alloyed layers were cut for metallographic analysis. The polished surfaces were etched using Keller's reagent. The chemical reaction between molten aluminium and the TiB<sub>2</sub> alloying powder led to the formation new phases in the matrix. The new phases formed were studied; the microstructures of the new phases were characterized by optical and scanning electron microscopes. The characteristics of the phases were studied by means of X-ray diffraction. An optical microscope was also used for microstructural analysis.

### Microhardness Test

The Vickers hardness of the alloyed cross sections was determined using a Matsuzawa Seiki microhardness tester. A through-thickness hardness profile was determined with a 150  $\mu\text{m}$  spacing between corresponding indentations with a load of 100 g. A minimum of five indents were made to obtain a good representation of the values obtained. The average microhardness value was calculated for the samples.

## Results and Discussion

### Powder Characterisation

Figure 1 shows the particle size distribution of the TiB<sub>2</sub> powder used for alloying. The average particle size was found to be -100 to 45  $\mu\text{m}$ .

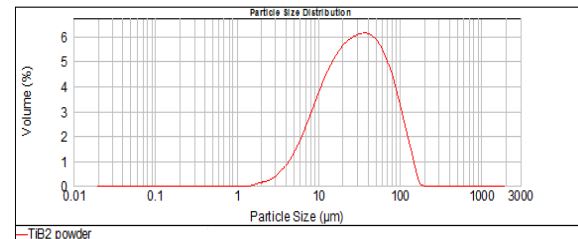


Figure 1: Particle size and distribution of TiB<sub>2</sub> powder

Figure 2 shows the XRD diffractograph of the powder. This shows that the powder used was pure and free from any contaminant. The peaks shown were that of Ti and TiB<sub>2</sub>. Figure 3 shows a SEM micrograph of the as received TiB<sub>2</sub> powder particles. The morphologies of the TiB<sub>2</sub> particles were irregular in shape and clustered together.

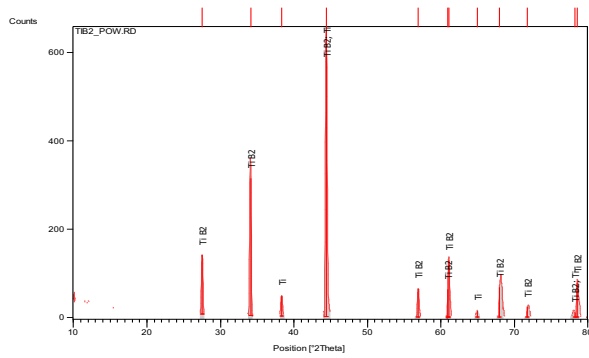


Figure 2: X-ray spectrum of  $TiB_2$  powder

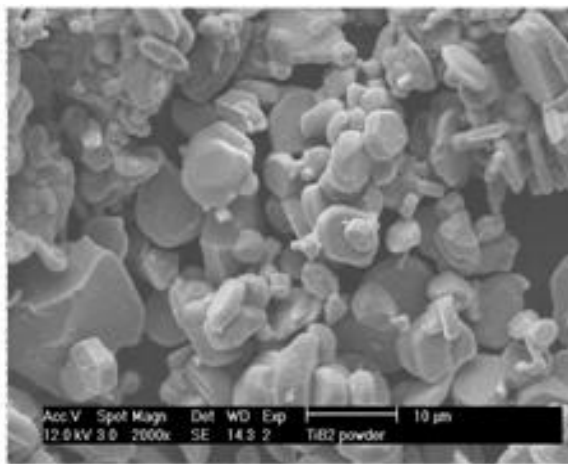


Figure 3: Scanning electron micrograph showing the microstructure of  $TiB_2$  powder

The X-ray diffractograph of the cross section of the AA 1200 can be seen in Figure 4. This shows the identified phases present in the Al; only aluminium peaks can be seen, an evidence of the purity of the substrate. The microhardness value of the AA 1200 is  $24.0 \pm 0.4$ .

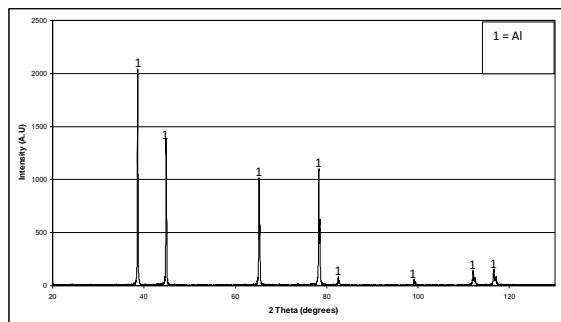


Figure 4: X-ray spectrum of AA 1200

### Microstructure of MMC

A typical stereo micrograph of the alloyed layer is shown in Figure 5.

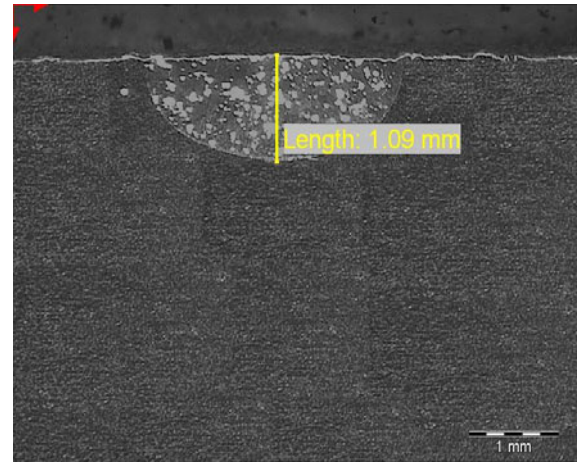


Figure 5: A typical stereo micrograph of an Al surface alloyed with  $TiB_2$

Uniform alloying (alloyed layer filled with powder) was achieved, evidence of good metallurgical bond between substrate and powder. The maximum depth of alloyed layer achieved was 1.17 mm representing approximately 20% of aluminium substrate thickness. The width of the single track is approximately equal to that of the laser beam of 3 mm for both samples.

Figures 6-7 shows the scanning electron micrographs of the cross section of the polished sample C laser alloyed. From these SEM results, micrographs consisted of the  $TiB_2$  powder well dispersed in the Al-matrix. The distribution of the  $TiB_2$  particles in the melt is by convection flow. The gray phases are  $TiB_2$  in the solidified Al-matrix. The metallurgical bonding existing between the substrate and the powder can be seen from the SEM micrograph. The same can be said for Sample D, Figures 8-9 also shows the SEM micrographs of these samples, bonding within the matrix are good. The EDS analysis for both samples C and D shows the presence of Al, Ti, B and O. The optical micrographs of the MMC layer for both samples confirmed that  $TiB_2$  particles are well dispersed in the Al-matrix.

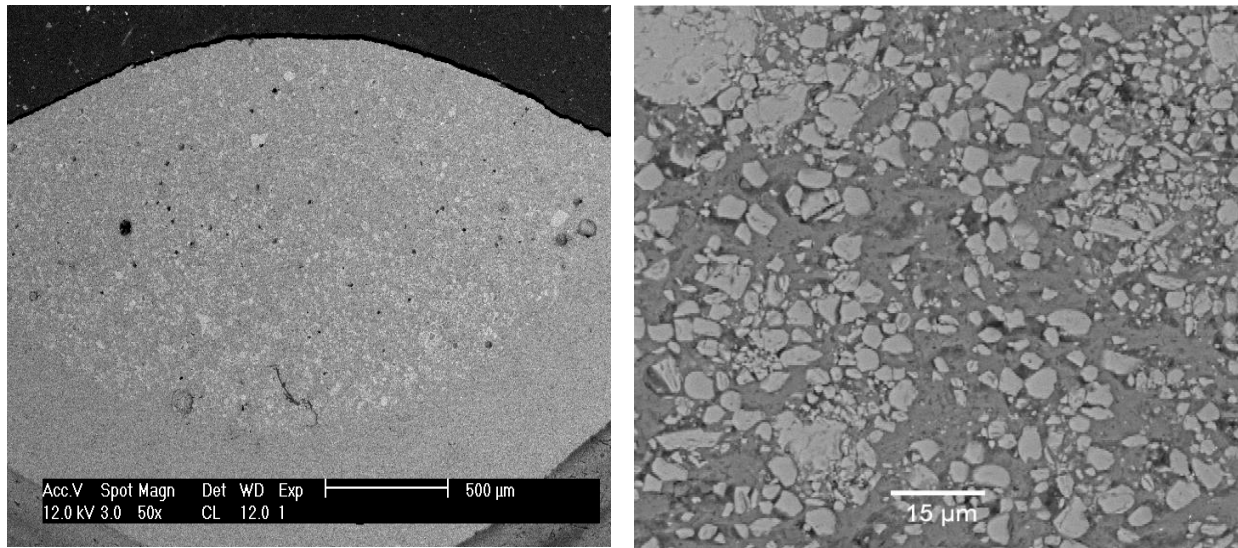


Figure 6: Scanning electron micrograph of sample C a laser formed composite surface of Al with  $TiB_2$  particles treated with 4 kW laser power, 0.6 m/min scan speed and 4 rpm powder feed rate at different magnification.

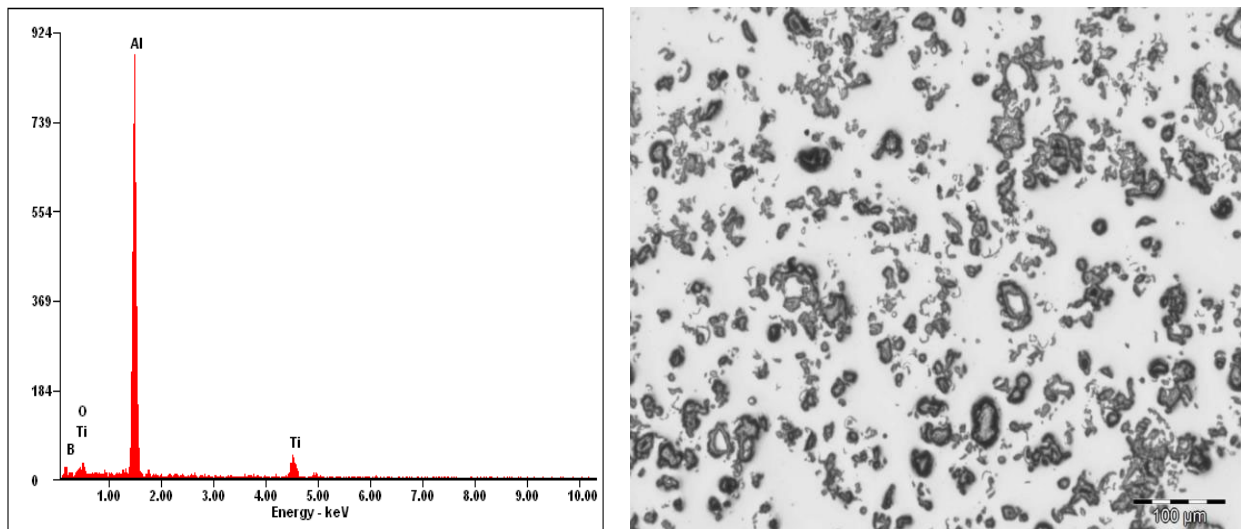


Figure 7: EDS analysis and the optical micrograph of sample C laser formed composite surface of Al with  $TiB_2$  particles treated with 4 kW laser power, 0.6 m/min scan speed and 4 rpm powder feed rate.

The particles of  $TiB_2$  can be seen to be fairly homogeneously distributed within the Al-matrix except for sample D where clustering of the powder can be seen from the SEM micrograph. A close comparison between the SEM micrographs of the samples revealed that the volume fraction of the  $TiB_2$  particles in the Al-matrix decreases with increase in the scan speed. It can be concluded that the laser

processing parameters used actually controlled the width of the melt pool, the quantity of powder deposited into it and hence the properties so modified. Sample D can be seen to have the lowest volume fraction of  $TiB_2$  while sample C has the highest volume fraction of powder corresponding to 0.6 m/min scan speed which is the lowest.

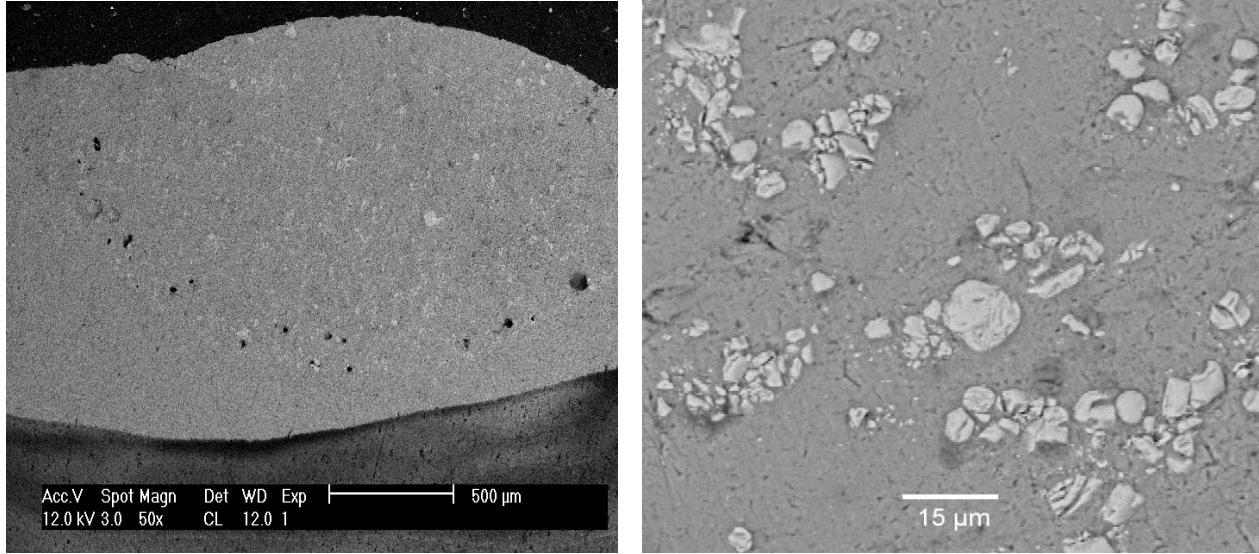


Figure 8: Scanning electron micrograph of sample D a laser formed composite surface of Al with  $\text{TiB}_2$  particles treated with 4 kW laser power, 1.0 m/min scan speed and 4 rpm powder feed rate at different magnification.

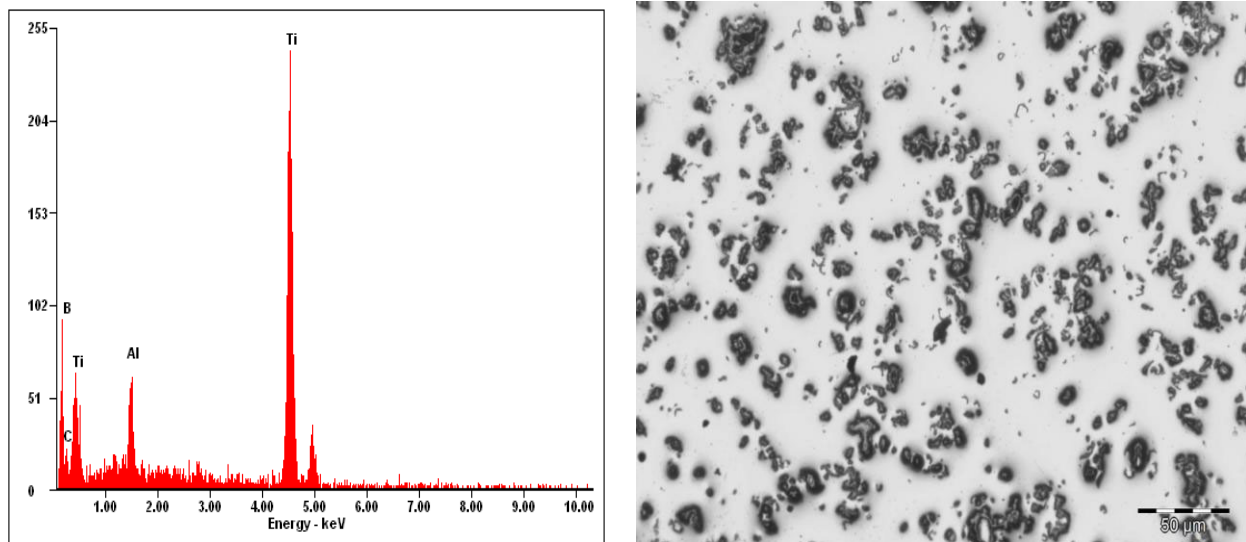


Figure 9: EDS analysis and the optical micrograph of sample D laser formed composite surface of Al with  $\text{TiB}_2$  particles treated with 4 kW laser power, 1.0 m/min scan speed and 4 rpm powder feed rate.

Figure 10 shows the XRD profiles for the samples C and D, from these profiles secondary phases were identified, phases present in the alloyed layer are:  $\text{TiB}_2$ ,  $\text{AlTi}$ ,  $\text{AlB}_2$ , Al, Ti, B. The Al and Ti belong to the same crystal system and the same space group, and as such their peaks are overlapping. The same for  $\text{TiB}_2$  and  $\text{AlB}_2$  – they belong to the same space group

and peaks are overlapping. However, the XRD result of sample D also showed the presence of  $\text{Al}_3\text{Ti}$ , this is an intermetallic phase that exhibits high hardness, high melting and also very brittle. This phase may be responsible for the higher hardness value exhibited by sample D.

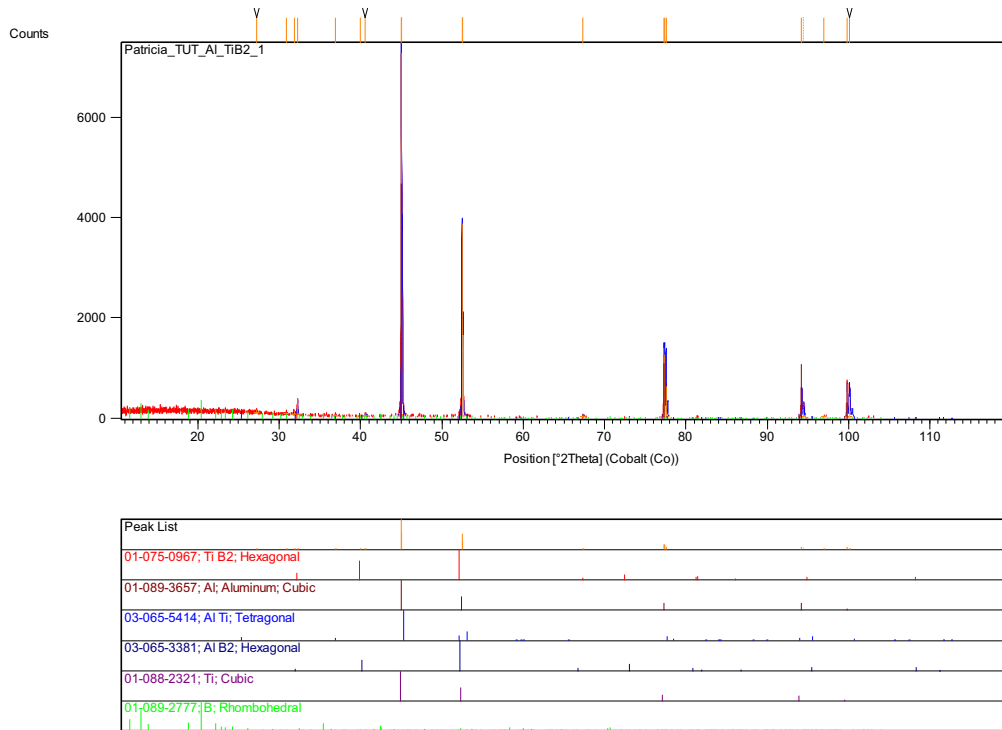


Figure 10: X-ray spectrum for the laser alloyed surfaces of Al with TiB<sub>2</sub>: sample C

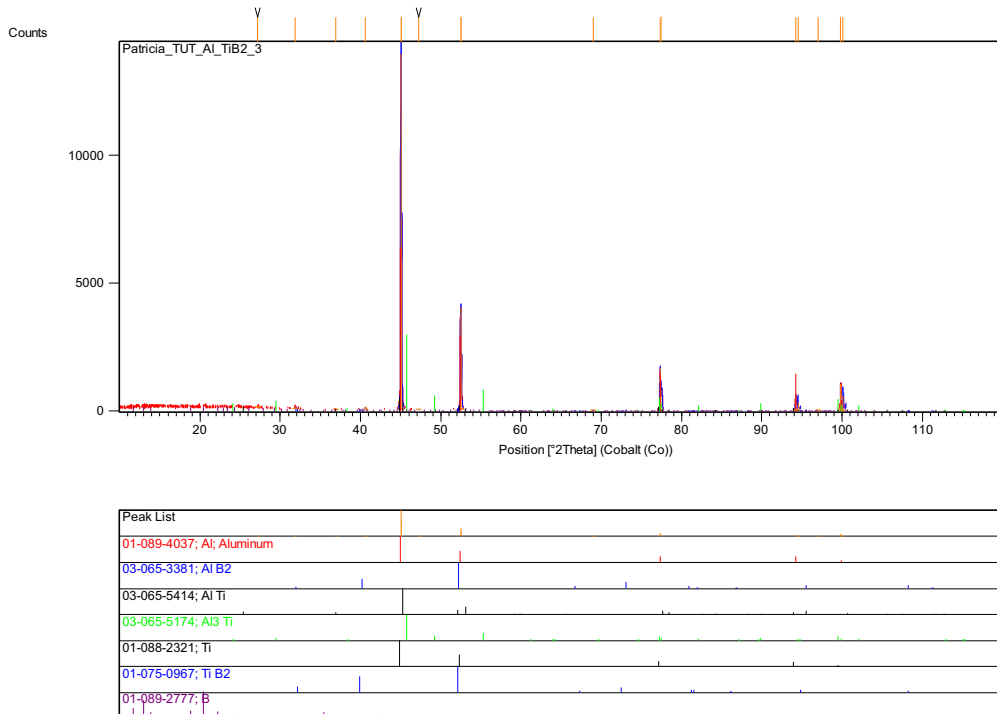


Figure 11: X-ray diffraction spectrums for the laser alloyed surfaces of Al with TiB<sub>2</sub>: sample D

### Microhardness Results

From Figure 12, laser alloying aluminium AA 1200 with  $TiB_2$  powder resulted in microhardness increase from  $24.0 \pm 0.4$  HV for base aluminium AA 1200 to approximately  $58.0 \pm 0.2$  HV for the alloyed layers. The microhardness profile data for all the samples shows significant fluctuation. The average microhardness values for all the samples were calculated, sample C has the highest value of microhardness, this is because of the  $Al_3Ti$  phase that was exhibited by this sample. This improvement in hardness (over double the microhardness of substrate) was attributed to the formation of MMC phases during alloying. The optimum laser processing parameter for the highest average

microhardness is laser power 4 kW, scan speed 1.0 m/min, powder feed rate 4 rpm. It can be concluded that the hardening using  $TiB_2$  powder is due to formation MMC as a result of the dispersion of the hard particles and that there exist an optimum volume fraction that will give the best microhardness property and also the presence of the  $Al_3Ti$  phase in the matrix is very vital.

Table 3 Properties of the alloyed layer

Sample label	C	D
Average microhardness value displayed by MMC (HV)	46.50	48.70
Depth of alloyed layer (mm)	1.17	1.09
Scan speed (m/min)	0.60	1.00

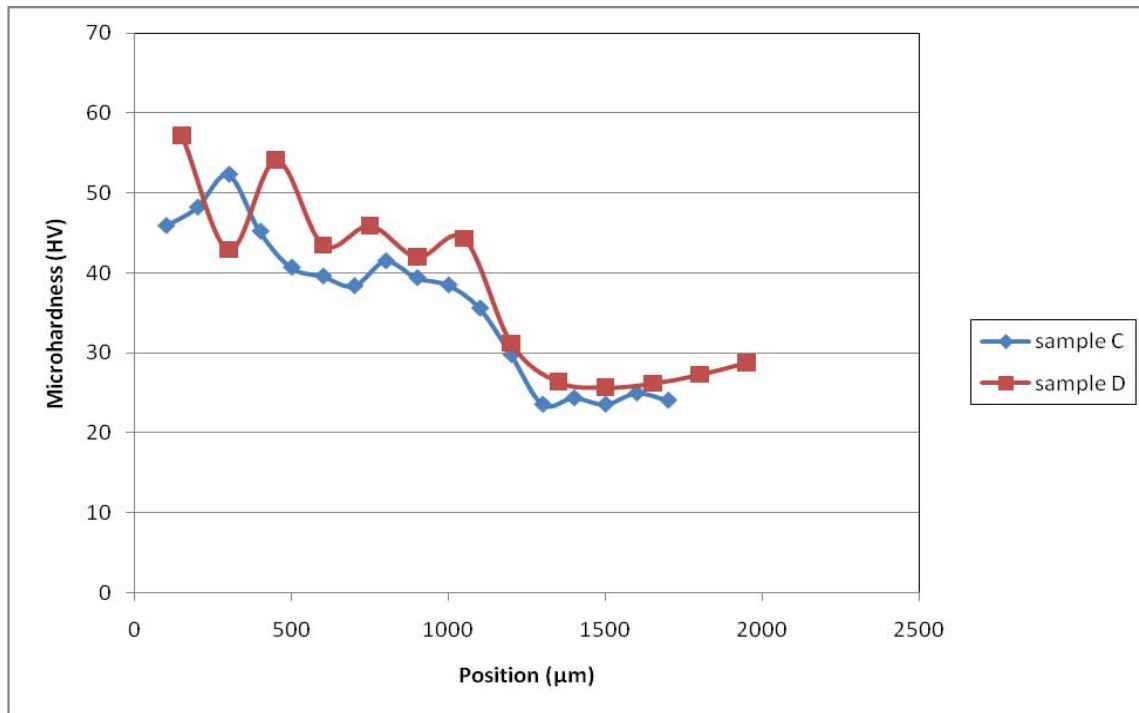


Figure 12: Microhardness profiles with depth for both samples

### Conclusions

Laser surface alloying of AA 1200 pure aluminium with  $TiB_2$  reinforcement using a 4.4 kW Sinar continuous wave Nd: YAG solid-state laser was successfully carried out. The resultant phases and hardness were investigated:

- A relationship exist between the laser processing parameters and volume fraction of powder deposited into the melt pool, the depth of alloyed layer and finally the microstructure and properties of the MMC formed.
- The increase in hardness from that of Al-substrate  $24 \pm 0.4$  to that of the alloy formed  $58.0 \pm 0.2$  is about twice that of substrate.

## References

- [1] Majumdar, J.D., Chandra, B.R., Nath, A.K. & Manna, I. (2006) In situ dispersion of titanium boride on aluminium by laser composite surfacing for improved wear resistance, *Surface & Coatings Technology* 201, 1236-1242.
- [2] Chen, Y. & Wang, H.M. (2006) Microstructure and wear resistance of laser-melted TiC reinforced nickel aluminide dual phase matrix in situ composite, *Intermetallics* 14, 325-331.
- [3] Man, H.C., Zhang, S., Yue, T.M. & Cheng, F.T. (2001) Laser surface alloying of NiCrSiB on Al6061 aluminium alloy, *Surface and Coatings Technology* 148, 136-142.
- [4] Chen, Y. & Wang, H.M. (2003) Microstructure and wear resistance of laser clad TiC reinforced FeAl intermetallic matrix composite coatings, *Surface and Coatings* 168, 30-36.
- [5] Staia, M.H., Cruz, M. & Dahotre, N.B. (2000) Microstructural and tribological characterization of an A-356 aluminium alloy superficially modified by laser alloying, *Thin Solid Films* 377-378, 665-674.
- [6] Pityana, S.L. (2009) Hardfacing of aluminium alloys by means of Metal Matrix Composites produced by laser surfacing alloying, in *Proceedings of LIM, Munich, Germany*, 439-444.
- [7] Davis, R.J. & Associates (1993) *Aluminium and aluminium alloys*, ASTM International Handbook Committee, 574-579.
- [8] Nurminen, J., Nakki, J. & Vuoristo, P. (2009) Microstructure and properties of hard and wear resistant MMC coatings deposited by laser cladding, *Int. Journal of Refractory Metals & Hard Materials* 27, 472-478.
- [9] Dubourg, L., Pelletier, H., Vaissiere, D., Hlawka, F. & Cornet, A. (1998) Mechanical characterisation of laser surface alloyed aluminium-copper systems, *Wear* 253, 119-126.

## Acknowledgements

The author would like to thank Tshwane university of Technology and CSIR- National Laser Centre for financial support of this work.

## Meet the Author

Patricia is a Metallurgist; she is a Lecturer and Section Head of the Department of Chemical and Metallurgical Engineering in Tshwane University of Technology, Pretoria, South Africa.